SECED 2023 Conference
*Earthquake Engineering & Dynamics for a Sustainable Future*
14-15 September 2023, Cambridge, UK

# DOUBLE-BAND APPROACH FOR SLOW-MOVING LANDSLIDES MONITORING

Mohammad Amin KHALILI[1], Luigi GUERRIERO[2], Chester SELLERS[3], Alessandro NOVELLINO[4], Domenico CALCATERRA[5], Diego DI MARTIRE[6]

**Abstract**: *Landslides are among the most devastating natural disasters globally, causing significant economic and environmental damage. The aim of this study was the use of two different Advanced Differential Interferometry SAR (A-DInSAR) approaches applied to double band SAR dataset for the overall reconstruction of mass movements affecting the southern sector of the city of Cuenca (Ecuador) where the buildings of the University of Azuay are located. The University of Azuay and highway infrastructure have been affected by slow-moving landslides since twenty years ago. A-DInSAR approaches are Small Baseline Subset (SBAS) and Permanent Scatterer Interferometry (PSI). The study area covers both urban and rural regions where mass movements occur. The central sector of phenomena is more evident because they are located in the urban area, while the upper sector is less obvious because it involves very vegetated areas. This study comprehensively analyses movements in and around The University of Azuay and compares two different A-DInSAR techniques based on different wavelengths of satellite radar images. The SBAS method works best in rural areas because it can work with distributed scatter (DS), while the PSI method is highly effective in urban areas because of finding stable scatterers (PS). To prepare the mean deformation rate map, two sets of radar images with different wavelengths: Sentinel 1 (C-band) and COSMO-SkyMed (X-band), ascending tracks, which penetration and measurements on green land are different at these double band SAR images. The time series analysis was conducted in the regions affected by landslides, and the periods of landslide activity were identified and compared with two GNSS positioning. The study appropriately identified the whole landslide's boundary and deformation kinematics by comparing and monitoring double-band SAR satellites and different processing techniques. The findings of this study can help develop better landslide hazard assessment and monitoring systems for disaster risk reduction strategies.*

***Keywords:*** *Landslides, PSI, SBAS, COSMO-SkyMed mission, Sentinel mission, GNSS, Cuenca*

## Introduction

Landslides are a significant geological phenomenon that affects many areas worldwide, causing damage to infrastructure and posing a significant risk to human life *(Ajmera and Tiwari, 2021; Lu* et al.*, 2021)*. With technological advancements, remote sensing and Earth-monitoring techniques have become more sophisticated, providing more accurate tools to study these natural phenomena *(Coda* et al.*, 2019; Valente* et al.*, 2021)*. These techniques have significantly addressed global challenges, such as deformation monitoring, disaster prevention, and risk assessment *(Ghorbanzadeh* et al.*, 2022; Petrucci, 2022)*.

Among the remote sensing techniques used to study landslide deformations, GNSS and Advanced-Differential Interferometry SAR (A-DInSAR) are two popular methods *(Atanasova-Zlatareva and Nikolov, 2017)*. GNSS stations in stable areas are used for spatial georeferencing

[1] Ph.D. Student, Federico II University of Naples, Department of Earth, Environmental and Resource Sciences, Naples, Italy, email address: mohammadamin.khalili@unina.it
[2] Dr, Federico II University of Naples, Department of Earth, Environmental and Resource Sciences, Naples, Italy,
[3] Dr, University of Azuay, IERSE, Cuenca, Ecuador
[4] Dr, British Geological Survey,England
[5] Dr, Federico II University of Naples, Department of Earth, Environmental and Resource Sciences, Naples, Italy,
[6] Dr, Federico II University of Naples, Department of Earth, Environmental and Resource Sciences, Naples, Italy,

and adjustment, while those affected by deformation are used to evaluate and compare to other monitoring techniques *(Bovenga* et al*., 2012; Foumelis et al.,2016; Soltanieh and Macciotta, 2022)*. Moreover, A-DInSAR can provide high spatial resolution and millimeter precision for determining the deformation rate map over a wide area *(Miele* et al*., 2021)*.

Over the years, several approaches have been developed to improve precision and accuracy in using SAR images. InSAR is a type of two-SAR image processing technique *(Gabriel et al.,1989)*, while A-DInSAR is a multi-SAR image processing technique. The differential principle can be combined with time series analyses, such as Smal BAseline Subset *(SBAS - Berardino* et al*., 2002; Hooper, 2008)* and Permanent Scatterers Interferometry *(PSI - Ferretti et al.2001)*. Each method has its benefits and drawbacks when retrieving spatio-temporal aspects of surface deformations over short and long periods.

The study area is the University of Azuay, located in Cuenca, Ecuador, which is characterized by the presence of diffuse mass movements, as witnessed by the numerous damages to the buildings present (Sellers *et al.*, 2021a). Previous studies have indicated that landslides in this area affect two different contexts: urban and rural areas (Sellers et al.,2021b). These variations in the type of area affected by landslides highlight the importance of using multiple approaches and types of SAR images to obtain a comprehensive understanding of the behavior of landslides in the region.

The SBAS technique utilizes a series of interferograms characterized by small spatio-temporal baselines. This technique retrieves time-series cumulative deformation using distributed scatterers (DS) *(Lanari* et al*., 2004)*, which are more available in rural areas. In contrast, the PSI technique measures deformation over Permanent Scatterers (PS), which are prevalent and denser in urban environments *(Guerriero* et al*., 2019)*. Due to their backscattering capabilities, buildings operating as natural reflectors allow images to remain coherent. Compared to PSI, the SBAS method uses DS pixels with shorter time coherence behavior, making it suitable for investigating and analyzing displacements in rural areas.

C- and X-band imagery acquired in the Sentinel 1-A (S1-A) and COSMO-SkyMed (CSK) missions are satellite products that are particularly appropriate for retrieving deformation data of landslides under urban and rural areas due to their high spatial resolution and short revisiting time of acquisition *(Bovenga* et al*., 2012; Fiaschi* et al*., 2017)*. X-band SAR images can capture detailed deformation thanks to the higher ground resolution (3 x 3 meters), while C-band SAR images have a better temporal resolution but a lower spatial resolution (20 x 4 meters). In this study, S1-A and CSK radar images were processed utilizing SBAS and PSI approaches and then compared to two GNSS stations located in the area affected by the deformation to better recognize the boundary of the slow-moving landslide kinematic.

The results of this study revealed that using different processing techniques (SBAS and PSI) and different SAR images by means of the double band can help to investigate and analyze the kinematics of landslides more effectively and accurately in both urban and rural areas. The study identified various deformation patterns in the area affected by the landslide, and the findings could be used to monitor the area and implement preventive measures to mitigate the risks.

## Case Study

The University of Azuay's main campus is located in the southern part of the city of Cuenca, characterized by an average elevation of 2,580 meters above sea level. Regarding the geological setting, colluvial and alluvial deposits, Turi and the Mangan formation are outcropped. The area experiences variable climatic conditions, including dry periods between June and November and high precipitation levels between December and May, with an annual average of 940 mm *(Sellers et al., 2021b)*.

The Tarqui formation is dominated by slightly consolidated and altered volcanic deposits, primarily consisting of Pyroclasts ranging from rhyolitic to andesitic tuffs *(Noblet et al., 1988)*, volcanic ash, and ignimbrites. The thickness of the formation reaches 1200 meters, with fossil wood ages around 25,000 and 34,000 years, indicating the Upper Pleistocene's age *(Steinmann, 1997)*. The Mangan Formation comprises three units, with a maximum thickness of 1,000 to 1,200 meters

preserved in the west-central part of the basin. This formation is in the Upper Miocene to Pliocene ages *(Sheppard, 1934; Hall and Calle, 1982; Steinmann, 1997)*.

The campus is classified as a hazardous area, as reported on the PRECUPA map (Sellers et al., 2021a), due to the presence of rocks such as clay and sandstone and a large amount of water. The area also has soil saturation levels above eight meters, which have triggered displacements affecting specific structures such as buildings, highway facilities, and civil works on the campus *(Sellers et al.,2021b)*. The study identified various deformation patterns in the area affected by the landslide, and the findings could be used to monitor the area and implement preventive measures to mitigate the risks.

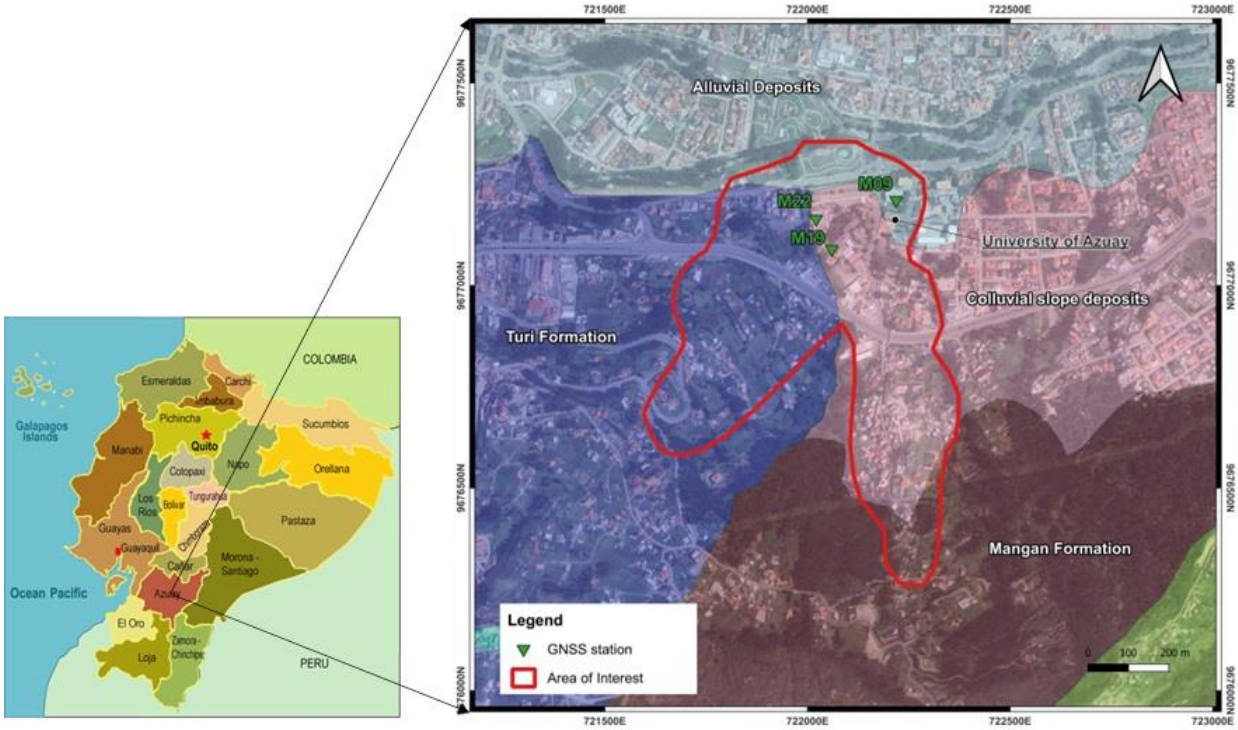


*Figure 1. Geological sketch map of the case study, showing the boundary of the mass movements and the location of three GNSS stations.*

## Data Sets

This study utilized C- and X-band imagery acquired from the S1-A and CSK missions. These satellite products provided the advantage of significant spatial resolution and short revisiting time, making them particularly suitable for deriving deformation data from our case study landslides in urban and rural areas.

S1-A is part of the Copernicus program conducted by the European Commission in collaboration with the European Space Agency (ESA). It is an imaging SAR mission operating in the C-band. The study utilized the S1-A radar images acquired between January 10, 2015, and November 26, 2018, comprising 61 SLC images.

In addition, CSK was commissioned and funded by the Italian Space Agency and the Italian Ministry of Defense. A constellation of four medium-sized low-Earth orbit satellites is deployed, each equipped with a high-resolution multi-mode SAR sensor operating in the X-band. Depending on the availability of all four satellites (i.e., CSKS1, …, CSKS4), the CSK constellation can be revisited between 8 and 16 days. CSK launched its first satellite in June 2007, and the whole system has been operational since 2011. Fifty-seven images were acquired over an ascending geometry track between March 12, 2016, and January 13, 2018, with a 40 x 40 km footprint used in this study. An overview of the acquired images can be found in Table 1.

| **Information** | **S1-A** | **CSK** |
|---|---|---|
| Acquisition Time | January 10th, 2015,<br>November 26th, 2018 | March 12th, 2016,<br>January 13th, 2018 |

| Type | SLC | SLC |
|---|---|---|
| Images (Nr) | 61 | 57 |
| Swath | IW2 | - |
| Pass | Ascending | Ascending |
| Central Look Angle (°) | 38 | 32 |
| Polarization | VV | HH |

*Table 1. Specifications of the S1-A and CSK acquisitions.*

GNSS stations are part of a global network of ground-based receivers that use signals from a constellation of satellites to determine their precise location on the Earth's surface. These stations are used for various applications, including surveying, navigation, and scientific research. They play an essential role in geodetic and geophysical studies by providing highly accurate positioning information, which measures ground deformation caused by various natural phenomena such as landslides. The data obtained from GNSS stations establish a reference frame that allows us to measure and compare the movements of the Earth's surface over time. In this study, the GNSS station was used for spatial coordination and adjustment of the deformation measurements obtained from the SAR images and for validating the results obtained from the SAR image processing techniques. In this study, we use continuous (or high-rate) data which is collected at a high sampling rate (1 Hz or higher) and provide a time series of raw GNSS observables to obtain a time series of GNSS observables, such as carrier phase, that can be used for precise positioning and displacement analysis. We monitor the data every month with one-hour sessions to ensure the accuracy and consistency of the data over time. The continuous GNSS data was processed using Trimble Business Center for monitoring and analysis. This powerful software offers a range of tools and capabilities for surveying and geospatial data management.

## Methodology

*SAR Data Processing*

The A-DInSAR has been widely used to measure ground motion caused by various natural phenomena, such as subsidence, landslides, earthquakes, and volcanic activity, as well as to monitor structures and infrastructure (Soltanieh and Macciotta, 2022). Among the different A-DInSAR approaches, in this study, PSI (Fetterri et al.,2001) and SBAS (Berardino et al., 2002, Lanari *et al.*, 2004) have been implemented. PSI relies on analyzing PS points, which are stable and persistent reflectors in the study area, to derive deformation measurements with high precision and spatial resolution. SBAS, on the other hand, utilizes a series of interferograms with small spatio-temporal baselines to derive time-series cumulative deformation using DS. Both PSI and SBAS can considerably improve the precision and accuracy of deformation rate maps and time series, with the rate maps and time series having an accuracy of approximately 1-2 mm/year and 5-10 mm, respectively (Colesanti and Wasowski, 2006).

*PSI*

The PSI technique is widely used for measuring ground deformation and displacement rates (Crosetto *et al.*, 2016). It is based on identifying PS points, which are radar targets characterized by high stability over time and high interferometric coherence, making them virtually immune to geometric and temporal interferometric effects. This study used the PSI technique to analyze the CSK images acquired between March 12, 2016, and January 13, 2018. The data were processed using the Coherent Pixels Technique – Temporal Phase Coherence (CPT-TPC) (Mora et al.,2003), identifying all possible interferogram pairs with spatial baselines lower than 300 meters. A TPC threshold of 0.7 was set to select the points for further analyses. The line of sight (LoS) of the displacement rate map and time series were elaborated, providing a high-precision view of the deformation caused by the landslides in the study area. The Digital Elevation Model (DEM) used to implement this technique had a cell resolution of 10 m x 10 m, and a multi-looking factor was considered 3 x 3 in range and azimuth, respectively. More details can be found in Sellers et al., 2021a

*SBAS*

The SBAS technique implemented in this study is a powerful approach for measuring ground deformations using S-1A data. The parameters used for this method were carefully chosen to optimize the results (Berardino *et al.*, 2002).

The SBAS method in the ISCE package (Rosen *et al.*, 2011) was implemented using several steps, starting with data preprocessing and ending with generating displacement maps and time series. The first step was the co-registration of the S1-A images using the precise orbit files provided by the European Spatial Agency. After co-registration, the images were resampled to a typical grid to enable interferometric processing. The next step was interferogram generation, where all possible pairs of images were used to create interferograms. In the SBAS approach, only a subset of these interferograms was selected based on the baseline values to minimize temporal decorrelation effects. The resulting interferograms were then filtered to remove residual noise and atmospheric disturbances. After filtering, the differential interferograms were unwrapped to obtain the phase information, which was then converted to LoS displacement values. The unwrapped phase values for each pixel were analyzed over time to obtain the displacement time series. Finally, the displacement values were geocoded to generate displacement maps.

During the unwrapping phase, the Snaphu software (Kampes, Hanssen, and Perski, 2004) has been used. The Snaphu threshold of 0.05 and the geocode threshold of 0.05 were selected to minimize noise and ensure high-quality interferograms. The spatial baseline orthogonal to the LoS was set at 100 meters, and the temporal baseline at 90 days, which were chosen to ensure the detection of deformation patterns with different spatial and temporal scales. The DEM used in this method had a cell resolution of 10 meters × 10 meters, which is suitable for identifying small-scale topographic features. Additionally, multi-looking with a factor of 3 × 9 was applied to the co-registered images to improve the coherence and reduce noise. The method produced a total of 234 interferogram pairs, which were used to generate the LoS mean displacement rate map and time series of displacement. It is worth noting that this method was applied to the S1-A images, which offer high spatial resolution and short revisit times, making them suitable for monitoring ground deformations in detail. Overall, implementing the SBAS method with carefully selected parameters allowed for accurately measuring ground deformations in the study area.

*Evaluation by GNSS Stations*

To obtain a time series of the relative positions of the receivers for analyzing displacement behavior caused by landslides, we processed continuous GNSS data using Trimble Business Center. Trimble Business Center allows us to easily import, process, and analyze GNSS data from various sources. With its intuitive user interface and advanced processing capabilities, we can perform various tasks such as network adjustment, baseline processing, and quality control checks. It also provides us with the ability to create and export reports, maps, and 3D models for further analysis and visualization. Using Trimble Business Center, we can ensure that the GNSS data we collect is processed and analyzed accurately and efficiently. With this powerful software tool, we can obtain precise positions and time series of GNSS observables that can be used for displacement analysis and other geospatial applications.

By comparing the processed Trimble Business Center (*Trimble Business Center* | *Trimble Geospatial*) observations from each receiver and applying differential corrections for atmospheric effects and other errors, it is possible to derive a time series of the receivers over time for evaluating results obtained by different A-DInSAR techniques. We can then compare these results with the GNSS dataset.

To ensure a meaningful comparison between InSAR-derived results and GNSS data, it is essential to ensure that both datasets are referenced to the same geodetic datum (i.e., the same reference point). This is because both InSAR and GNSS measurements are sensitive to the Earth's surface deformation, and the deformation can be expressed in different reference frames depending on the chosen datum.

In this case, we have three GNSS stations, and the M09 station was located in the stable area. Therefore, we geo-referenced CSK and S1-A according to this station separately using the M09 station's data. By referencing both our InSAR and GNSS datasets to the same reference point, we could make a meaningful comparison between the other two GNSS stations, with the location highlighted in Fig. 1.

To compare the A-DInSAR-derived results with the GNSS data, the displacement time series were interpolated to the same time series as the GNSS observations using a linear interpolation method. The GNSS observations were then subtracted from the interpolated A-DInSAR time series to obtain the residuals.

## Results and Discussion

*Time Series of S1-A Cumulative Displacement*

The time series cumulative displacement figure obtained from the SBAS technique processing of S1-A images in the ISCE package illustrated a clear deformation pattern in the University of Azuay landslides area. The shift was observed as early as May 2016, with a significant acceleration in July 2017 and finally in May 2018 until the end of processing in November 2018. It is important to note that the negative values confirm the direction of the deep slope of the area, which is in the SW-NE direction. The deformations were mainly positive and near zero in the southern, eastern, and northeastern parts, with up to nearly 6 cm of deformation from the eastern part to the southeastern part.

In contrast, the western part to the north and north-western had negative deformation in the LoS direction, starting on July 10, 2017, and then moved to the center and west of the region. The maximum deformation of nearly 8 cm was recorded on June 11, 2018, and continued until November 26, 2018. The spatial heterogeneity of the deformation of the University of Azuay landslide was evident, with the most considerable deformation in the middle to the west part of the landslide, followed by the landslide toe and deformation at the landslide crown (Figure 2).

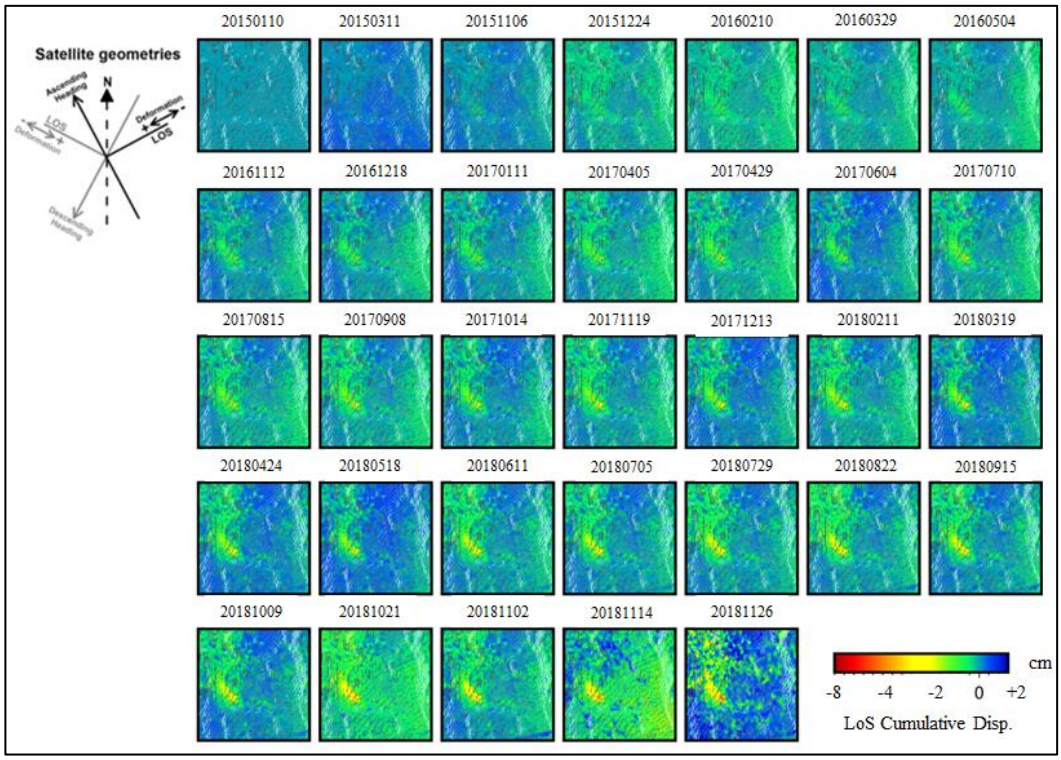


*Figure 2. The time-series cumulative deformation maps along the LoS according to the SBAS technique (S1-A).*

The time series cumulative deformation obtained from the SBAS technique processing of S1-A images has provided essential information on the deformation behavior of the University of Azuay landslides. The analysis of the cumulative deformation map (Figure 2) has helped to identify the most critical areas of deformation, which could aid in mitigating the landslide's potential hazards. The map's ability to show the direction and magnitude of deformation over time provides a comprehensive understanding of the landslide's behavior, making it helpful in monitoring its evolution. The time series cumulative deformation map obtained from the SBAS technique processing of S1-A images has proved to be an effective tool for monitoring the behavior of landslides and can be used in conjunction with other monitoring techniques, such as GNSS and

field observations, to improve the understanding of the landslide's behavior and to develop effective mitigation strategies.

*Mean Deformation Rate Map*

This study analyzed the mean deformation rate of the University of Azuay landslides using PSI and SBAS techniques in the radar LoS direction applied to S1-A and CSK images, respectively. The results demonstrate that the mean deformation rate of the University of Azuay landslides in the LoS direction ranges from -1 to -9 cm/year, with the mean velocity along the LoS ranging from -9 to +7 cm/year in the central to the east sector of the study area in both CSK and S1-A images (Figure 3). This information is critical for understanding the landslides' behavior and predicting future movement.

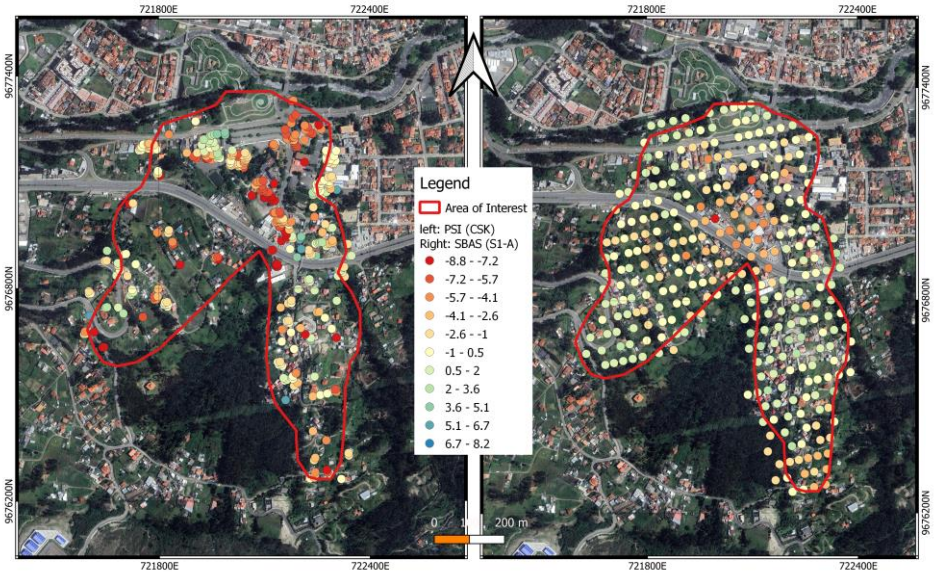


*Figure 3. The mean deformation rate maps along the LoS according to the left) PSI (CSK), and right) SBAS (S1-A).*

During the processing of CSK images between March 12, 2016, and January 13, 2018, most of the deformation was observed in the central part of the case study area, ranging from -9 to -2 cm/year. The S1-A images were processed to illustrate the complete landslides from January 10, 2015, to November 26, 2018, with ranges from -7 to -1 cm/year. These results provide an understanding of how the landslides in the study area developed over time and indicate that the deformation in Azuay University and the highway near the center of the study area were covered.

The PSI method failed to detect PSs in the CSK images related to the highway section, which did not display deformations. The SBAS technique covered the remaining deformation effects resulting from the landslides, which ranged from -8 to -1 cm/year due to the presence of DSs in the processed S1-A images. This highlights the importance of utilizing multiple techniques to obtain accurate and comprehensive data for landslide monitoring and analysis.

The landslide deformation is mainly concentrated in the middle, with a longitudinal length of approximately 600-700 m. The upper and lower sectors did not display significant movements, except for the upper sector of the southern slope, where values lower than -2 cm/year were observed, and deformation did not change significantly. These findings provide important insights into the distribution of deformation and can help improve understanding of the landslide kinematics in the study area, which is critical for developing effective strategies for hazard management and disaster mitigation.

In conclusion, combining the PSI and SBAS techniques provided valuable insights into the deformation behavior of the University of Azuay landslides in the study area. The analysis of the mean deformation rate, the distribution of deformation, and the movement patterns and their changes over time are essential for understanding landslide kinematics and developing effective strategies for hazard management and disaster mitigation. The use of multiple techniques, such as SBAS and PSI, can enhance the accuracy and reliability of the data and provide a more comprehensive view of the behavior of the landslides over time.

*Evaluation by GNSS Stations*

The comparison between the GNSS and A-DInSAR time series provides valuable insights into the displacement behavior caused by the landslides in the study area. The GNSS 3D measurements were projected to the same reference date along the LoS as the A-DInSAR time series to ensure a proper and effective investigation of the landslide-induced displacement. A spline interpolation matched the GNSS and A-DInSAR time series to a typical period. The comparison was initially performed for the two GNSS time series between 2016 and 2018. Results show that the GNSS time series agree with the A-DInSAR time series, as demonstrated in Figure 4.

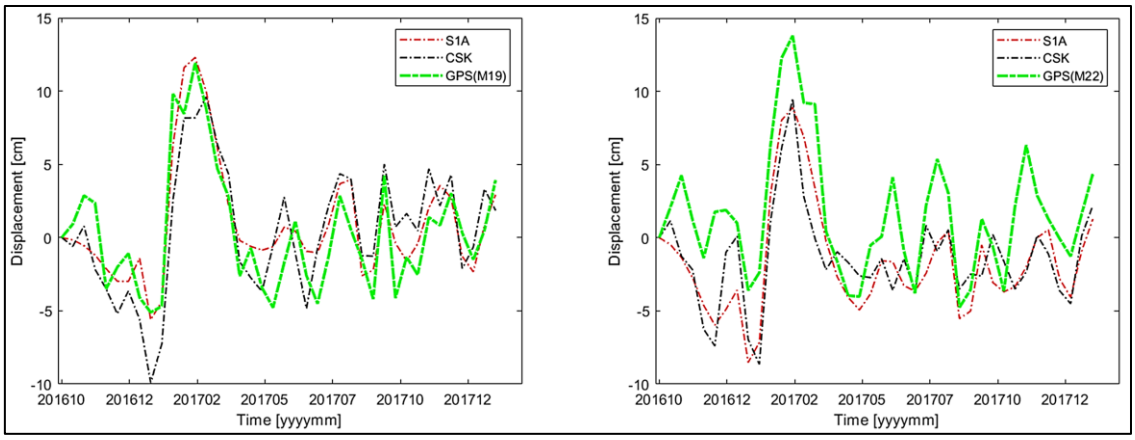


*Figure 4. Comparison of GNSS and InSAR time-series derived from S1-A and CSK data at GNSS station M22 (Right plot), M19 (Left plot).*

The cumulative displacements obtained from the SBAS technique with C-band images are more similar in behavior to the cumulative displacements obtained from the two GNSS stations. Even though the total period in the GNSS stations is close to zero displacements, the accuracy of the work done with both techniques and both types of SAR images confirm periodic deformation behaviors due to seasonal rainfall from November to February. These findings support the validity and reliability of the cumulative displacement data obtained from the SBAS technique and the C-band images in investigating landslide-induced deformation.

The agreement between the GNSS and A-DInSAR time series is critical for understanding the kinematics of the landslides in the study area. This comparison enables researchers to identify and analyze periodic deformation behavior, essential for understanding the deformation patterns and predicting future deformation in the area.

## Conclusion

The results of this study demonstrate that there are significant displacement rates in the study area. Multiple movements were identified in the northern and northeastern parts of the area, including in urban areas. The highest displacement rates were found in the vicinity of Azuay University and the nearby highway. Meanwhile, the central part of the study area, which contains rural areas, was also affected by the landslide. In contrast, other landslide areas showed no deformation, which can help us better understand the shape of the landslide.

Comparing the results with two GNSS stations showed excellent agreement between the radar image processing and GNSS results, confirming the accuracy and reliability of the analysis. The cumulative deformation results also provided valuable information for further analysis. It should be noted that the PSI technique with CSK images did not capture the complete deformation patterns of the landslide, and the SBAS technique with S1-A images provided a more complete analysis.

Using different techniques and double-band SAR images allowed a more accurate analysis of the landslide kinematics in the study area. This highlights the importance of using multiple data sources and processing techniques to obtain accurate results.

In conclusion, this study provides important insights into the study area's displacement rates and deformation patterns of landslides. The findings suggest that different techniques and multiple

data sources are necessary for accurately analyzing and monitoring landslides, especially in areas with both urban and rural types. The results also suggest that geological formations can play a critical role in investigating landslides, and a better understanding of these formations can aid in identifying and analyzing landslide kinematics.

## References

Ajmera, B. and Tiwari, B. (2021) 'Recent Advances in the Methods of Slope Stability and Deformation Analyses', in B. Tiwari et al. (eds) Understanding and Reducing Landslide Disaster Risk: Volume 4 Testing, Modeling and Risk Assessment. Cham: Springer International Publishing (ICL Contribution to Landslide Disaster Risk Reduction), pp. 81–108. Available at: https://doi.org/10.1007/978-3-030-60706-7_5.

Atanasova-Zlatareva, M. and Nikolov, H. (2017) 'Displacements Monitoring Of The Trifon Zarezan Landslide By Gnss Observations And Insar Introduction', in. 9th Congress of the Balkan Geophysical Society, European Association of Geoscientists & Engineers, pp. 1–5. Available at: https://doi.org/10.3997/2214-4609.201702567.

Berardino, P. et al. (2002) 'A new algorithm for surface deformation monitoring based on small baseline differential SAR interferograms', IEEE Transactions on Geoscience and Remote Sensing, 40(11), pp. 2375–2383. Available at: https://doi.org/10.1109/TGRS.2002.803792.

Bovenga, F. et al. (2012) 'Using COSMO/SkyMed X-band and ENVISAT C-band SAR interferometry for landslides analysis', Remote Sensing of Environment, 119, pp. 272–285. Available at: https://doi.org/10.1016/j.rse.2011.12.013.

Coda, S. et al. (2019) 'Uplift Evidences Related to the Recession of Groundwater Abstraction in a Pyroclastic-Alluvial Aquifer of Southern Italy', Geosciences, 9(5), p. 215. Available at: https://doi.org/10.3390/geosciences9050215.

Colesanti, C. and Wasowski, J. (2006) 'Investigating landslides with space-borne Synthetic Aperture Radar (SAR) interferometry', Engineering Geology, 88(3), pp. 173–199. Available at: https://doi.org/10.1016/j.enggeo.2006.09.013.

Crosetto, M. et al. (2016) 'Persistent Scatterer Interferometry: A review', ISPRS Journal of Photogrammetry and Remote Sensing, 115, pp. 78–89. Available at: https://doi.org/10.1016/j.isprsjprs.2015.10.011.

Ferretti, A., Prati, C. and Rocca, F. (2001a) 'Permanent scatterers in SAR interferometry', IEEE Transactions on Geoscience and Remote Sensing, 39(1), pp. 8–20. Available at: https://doi.org/10.1109/36.898661.

Ferretti, A., Prati, C. and Rocca, F. (2001b) 'Permanent scatterers in SAR interferometry', IEEE Transactions on Geoscience and Remote Sensing, 39(1), pp. 8–20. Available at: https://doi.org/10.1109/36.898661.

Fiaschi, S. et al. (2017) 'From ERS-1/2 to Sentinel-1: two decades of subsidence monitored through A-DInSAR techniques in the Ravenna area (Italy)', GIScience & Remote Sensing, 54(3), pp. 305–328. Available at: https://doi.org/10.1080/15481603.2016.1269404.

Foumelis, M., Papageorgiou, E. and Stamatopoulos, C. (2016) 'Episodic ground deformation signals in Thessaly Plain (Greece) revealed by data mining of SAR interferometry time series', International Journal of Remote Sensing, 37(16), pp. 3696–3711. Available at: https://doi.org/10.1080/01431161.2016.1201233.

Gabriel, A.K., Goldstein, R.M. and Zebker, H.A. (1989) 'Mapping small elevation changes over large areas: Differential radar interferometry', Journal of Geophysical Research: Solid Earth, 94(B7), pp. 9183–9191. Available at: https://doi.org/10.1029/JB094iB07p09183.

Ghorbanzadeh, O. et al. (2022) 'The Outcome of the 2022 Landslide4Sense Competition: Advanced Landslide Detection From Multisource Satellite Imagery', IEEE Journal of Selected Topics in Applied Earth Observations and Remote Sensing, 15, pp. 9927–9942. Available at: https://doi.org/10.1109/JSTARS.2022.3220845.

Guerriero, L. et al. (2019) 'PS-driven inventory of town-damaging landslides in the Benevento, Avellino and Salerno Provinces, southern Italy', Journal of Maps, 15(2), pp. 619–625. Available at: https://doi.org/10.1080/17445647.2019.1651770.

Hall, M.L. and Calle, J. (1982) 'Geochronological control for the main tectonic-magmatic events of Ecuador', Earth-Science Reviews, 18(3), pp. 215–239. Available at: https://doi.org/10.1016/0012-8252(82)90038-1.

Hooper, A. et al. (2004) 'A new method for measuring deformation on volcanoes and other natural terrains using InSAR persistent scatterers', Geophysical Research Letters, 31(23). Available at: https://doi.org/10.1029/2004GL021737.

Hooper, A. (2008) 'A multi-temporal InSAR method incorporating both persistent scatterer and small baseline approaches', Geophysical Research Letters, 35(16). Available at: https://doi.org/10.1029/2008GL034654.

Kampes, B.M., Hanssen, R.F. and Perski, Z. (2004) 'Radar Interferometry with Public Domain Tools', 550, p. 10.

Lanari, R. et al. (2004) 'A small-baseline approach for investigating deformations on full-resolution differential SAR interferograms', IEEE Transactions on Geoscience and Remote Sensing, 42(7), pp. 1377–1386. Available at: https://doi.org/10.1109/TGRS.2004.828196.

Lu, Y. et al. (2021) 'Mechanism and Stability Analysis of Deformation Failure of a Slope', Advances in Civil Engineering, 2021, p. e8949846. Available at: https://doi.org/10.1155/2021/8949846.

Miele, P. et al. (2021) 'Landslide Awareness System (LAwS) to Increase the Resilience and Safety of Transport Infrastructure: The Case Study of Pan-American Highway (Cuenca–Ecuador)', Remote Sensing, 13(8), p. 1564. Available at: https://doi.org/10.3390/rs13081564.

Noblet, C., Lavenu, A. and Schneider, F. (1988) 'Etude géodynamique d'un bassin intramontagneux tertiaire sur décrochements dans les Andes du Sud de l'Equateur : l'exemple du bassin de Cuenca', in. Available at: https://www.semanticscholar.org/paper/Etude-g%C3%A9odynamique-d'un-bassin-intramontagneux-sur-Noblet-Lavenu/70f785de5cc050b47f1a132aa6217b5c6210dc68 (Accessed: 29 January 2023).

Petrucci, O. (2022) 'Landslide Fatality Occurrence: A Systematic Review of Research Published between January 2010 and March 2022', Sustainability, 14(15), p. 9346. Available at: https://doi.org/10.3390/su14159346.

Rosen, P.A. et al. (2011) 'InSAR Scientific Computing Environment - The Home Stretch', 2011, pp. IN42A-02.

Sellers, C. et al. (2021) 'Ground Deformation Monitoring of a Strategic Building Affected by Slow-Moving Landslide in Cuenca (Ecuador)', in P. Rizzo and A. Milazzo (eds) European Workshop on Structural Health Monitoring. Cham: Springer International Publishing (Lecture Notes in Civil Engineering), pp. 149–158. Available at: https://doi.org/10.1007/978-3-030-64908-1_14.

Sellers, C.A., Buján, S. and Miranda, D. (2021) 'MARLI: a mobile application for regional landslide inventories in Ecuador', Landslides, 18(12), pp. 3963–3977. Available at: https://doi.org/10.1007/s10346-021-01764-9.

Sheppard, G. (1934) 'Geology of the Interandine Basin of Cuenca, Ecuador', Geological Magazine, 71(8), pp. 356–370. Available at: https://doi.org/10.1017/S0016756800093596.

Soltanieh, A. and Macciotta, R. (2022) 'Updated Understanding of the Thompson River Valley Landslides Kinematics Using Satellite InSAR', Geosciences, 12(10), p. 359. Available at: https://doi.org/10.3390/geosciences12100359.

Steinmann, M. (1997) The Cuenca Basin of Southern Ecuador: Tectono-sedimentary History and the Tertiary Andean Evolution : a Dissertation Submitted to the Swiss Federal Institute of Technology Zurich for the Degree of Doctor of Natural Sciences. Swiss Federal Institute of Technology Zurich.

Trimble Business Center | Trimble Geospatial (no date). Available at: https://geospatial.trimble.com/products-and-solutions/trimble-business-center (Accessed: March 9 2023).

Valente, E. et al. (2021) 'Studying a Subsiding Urbanized Area from a Multidisciplinary Perspective: The Inner Sector of the Sarno Plain (Southern Apennines, Italy)', Remote Sensing, 13(16), p. 3323. Available at: https://doi.org/10.3390/rs13163323.